One-pot hydrothermal synthesis of ZnO/RGO/ZnO@Zn sensor for sunset yellow in soft drinks

Xian Wu, Xiaojuan Zhang, Chongjun Zhao, Xiuzhen Qian

www.elsevier.com/locate/talanta

PII: S0039-9140(17)31210-9
DOI: http://dx.doi.org/10.1016/j.talanta.2017.12.005
Reference: TAL18141

To appear in: *Talanta*

Received date: 3 August 2017
Revised date: 27 November 2017
Accepted date: 2 December 2017

Cite this article as: Xian Wu, Xiaojuan Zhang, Chongjun Zhao and Xiuzhen Qian, One-pot hydrothermal synthesis of ZnO/RGO/ZnO@Zn sensor for sunset yellow in soft drinks, *Talanta,* http://dx.doi.org/10.1016/j.talanta.2017.12.005

One-pot hydrothermal synthesis of ZnO/RGO/ZnO@Zn sensor for sunset yellow in soft drinks

Xian Wu, Xiaojuan Zhang, Chongjun Zhao*, Xiuzhen Qian

Key Laboratory for Ultrafine Materials of Ministry of Education, Shanghai Key Laboratory of Advanced Polymeric Materials, School of Materials Science and Engineering, East China University of Science and Technology, Shanghai 200237, P.R. China, Tel: +86-21-6425 0838; Fax: +86-21-6425 0838; E-mail: chongjunzhao@ecust.edu.cn

*** Corresponding author:**

Chongjun Zhao

Key Laboratory for Ultrafine Materials of Ministry of Education,

Shanghai Key Laboratory of Advanced Polymeric Materials,

School of Materials Science and Engineering

East China University of Science and Technology

Shanghai 200237, P.R. China

Tel: 0086-21-6425 0838

Fax: 0086-21-6425 0838

E-mail: chongjunzhao@ecust.edu.cn

Abstract: ZnO/RGO/ZnO nanocomposite was *in-situ* anchored on Zn foil through a simple one-step hydrothermal approach. Based on the redox reaction between graphene oxide (GO) and Zn foil, and the electrostatic attraction between the negative-charged GO and positive-charged zinc ions, three strong interfaces of ZnO/RGO, RGO/ZnO and ZnO/Zn were simultaneously constructed, which led to improved electron and ion transfer. As-prepared ZnO/RGO/ZnO@Zn directly acted as sensor for amperometric detection of sunset yellow without further assembling, which exhibited an ultrahigh sensitivity of 20.25 uA·μM^{-1}·cm^{-2}, a low limit of detection (3 nM), a wide linear detection ranging from 0.01 to 5 μM.

Graphical abstract:

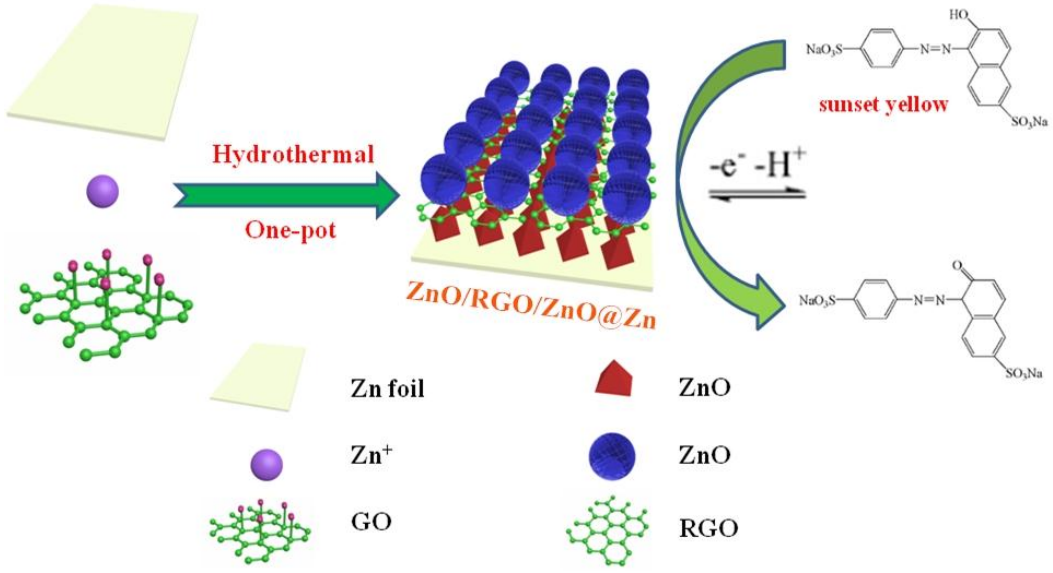

A ZnO/RGO/ZnO@Zn nanocomposite was *in-situ*-grown on Zn foil through a Zn foil-involved one-pot hydrothermal reaction. As-prepared ZnO/RGO/ZnO@Zn directly acted as a nonenzymatic sunset yellow sensor with an ultrahigh sensitivity, low detection limit and wide detection range.

Keywords: ZnO/RGO/ZnO; *In-situ* hydrothermal growth; Non-enzymatic biosensor; Sunset yellow

1. Introduction

Food safety is a worldwide public health problem. It is not only closely related to human health, but also seriously affects the development of society and economy. Nowadays, synthetic colorants additives are extensively applied in variety of foods due to so many advantages as high stability, low production cost, color uniformly and low microbiological contamination, which make foods more appetitive and attractive[1-4]. Among various types of synthetic colorants additives, sunset yellow plays an important role in food industry and acquire consumers' acceptance due to their superior physical and chemical properties. However, studies have shown that excessive consummation of sunset yellow maybe cause many diseases, such as asthmatic and allergy reaction, renal failure and attention deficit hyperactivity disorder (ADHD)[5-8].

Undoubtedly, it is essential to control the content of sunset yellow in food industry by preparing a simple, rapid and economic analysis method for food safety. Recently, various analytical methods have been applied to determine the content of sunset yellow, e.g., those techniques including spectrophotometry[9, 10] and high

performance liquid chromatography (HPLC)[6, 11] have been applied to detect sunset yellow. Unfortunately, there are some limitations of the above-mentioned techniques, including time-consuming, cost equipment as well as complicated pretreatment. In order to overcome the above disadvantages, many researchers turn their attention to the electrochemical analysis methods with high sensitivity, low cost and in situ detection [12-15]

The electrochemical sensors based on graphene and its nanocomposites have been reported for the detection of sunset yellow. Wang et al. fabricated a gold nanoparticles/graphene electrode for highly sensitive non-enzymatic electrochemical determination of sunset yellow[4]. Li et al. synthesized a new nanomaterial MGO/ β-CD/IL/AuNPs for non-enzymatic sunset yellow detection[16]. However, the utilization of gold nanoparticles will increase the cost of sensor. Gan et al. developed graphene-based composites with nickel nanoparticles[17], phosphotungstic acid hybrid[18] or mesoporous TiO_2[3] for the simultaneous determination of sunset yellow in food. However, the preparation of materials is relatively complicated and the above mentioned graphene-based nanocomposites have to suffer from loading on the surface of glassy carbon electrode (GCE), i.e., an electrode preparation process is necessary.

Herein, a zinc oxide/graphene-based and binder-free electrochemical non-enzymatic sensor is presented, which is sensitive to sunset yellow. This sensor consisting of ZnO/RGO/ZnO composites was in-situ grown on Zn foil surface through a one-step simple hydrothermal approach, i.e., both the synthesis and loading of ZnO/RGO/ZnO were simultaneously completed during the hydrothermal process. As-prepared ZnO/RGO/ZnO@Zn nanocomposite was directly utilized as the electrochemical sensor electrode, which exhibited excellent performances to the non-enzymatic sunset yellow sensing.

2. Experimental

2.1. Materials and reagents

Pristine graphite powder, hydrogen peroxide (H_2O_2, 30 wt%), hydrochloric acid (HCl, 36.0–38.0 wt%), sulfuric acid (H_2SO_4, 95–98 wt%), phosphorus pentoxide (P_2O_5), potassium permanganate ($KMnO_4$), ethanol (C_2H_5OH, >99.7 wt%), potassium persulfate ($K_2S_2O_8$), acetone (C_3H_6O, 99.5%), Zinc foil (Zn, 0.2 mm, 6 N), Sodium dihydrogen phosphate ($NaH_2PO_4{\cdot}2H_2O$, >99.0%), Disodium hydrogen phosphate dodecahydrate ($Na_2HPO_4.12H_2O$, >99.0%), Zinc nitrate ($Zn(NO_3)_2{\cdot}6H_2O$, 99.5%), were all purchased from Sinopharm Chemical Reagent Company(Shanghai, China, http://www.sinoreagent.com). And all chemical reagents were used as received without any further purification.

2.2. Preparation of ZnO/RGO/ZnO@Zn electrode

Zinc foil was cleaned with acetone, ethanol, and deionized water under ultrasound irradiation, respectively. Graphene oxide (GO) was prepared from pristine graphite powder based on a modified Hummer's method [19, 20].

ZnO/RGO/ZnO on Zn foil was prepared referring to the previous works on MxOy/RGO/MxOy[21-23]. GO (15 mg) was dispersed in 50 mL of deionized water by a sonication for 1 h, and 0.02 mmol $Zn(NO_3)_2 \cdot 6H_2O$ was added into the homogenous GO dispersion under continuously agitation followed by a sonication for 0.5 h. The obtained mixed solution was transferred into a Teflon-lined stainless steel autoclave (100mL). The cleaned Zn foil (0.5× 2 cm^2) was immersed in the solution and then suffered from a hydrothermal process at 150 ºC for 24 h. Subsequently, the treated Zn foil was washed with ethanol and deionized water respectively, and then dried in a vacuum oven at room temperature for 24 h. Finally, this obtained samples were denoted as ZnO/RGO/ZnO@Zn. The contrast samples of RGO/ZnO@Zn, ZnO@Zn and ZnO/ZnO@Zn were also prepared. The schematic illustration for the synthesis and electrochemical reaction mechanism of the ZnO/RGO/ZnO@Zn electrode was shown in Scheme.1.

2.3. Characterizations of ZnO/RGO/ZnO@Zn electrode

The crystalline structures of samples were performed by X-ray diffraction (XRD) of wide-angle (10°–80°, 40 kV/200 mA) using an X-ray diffractometer with Cu Kα radiation (λ = 1.5406 Å). The Raman spectra was carried out on an INVIA Raman microprobe (Renishaw Instruments, UK) with 514 nm laser excitation. The morphology and size of all samples were characterized using a field emission scanning electron microscope (FESEM, S4800) and a transmission electron microscope (TEM, JEM 2100, and JEM 2100F). The elementary composition of prepared products was performed by energy dispersive X-ray spectrometer (EDS, Bruker, AXS, Quantax 400-30).

2.4. Electrochemical performances of ZnO/RGO/ZnO@Zn electrode

All electrochemical measurements were taken on a CHI660E electrochemical workstation (CH Instruments, Shanghai, China) and in 0.2 M phosphate buffered solution(pH=7.0) with a conventional three-electrode system at room temperature. Synthesized ZnO/RGO/ZnO@Zn samples were directly used as working electrode, a saturated calomel electrode (SCE) as reference electrode, and the Pt foil (0.5×0.5 cm^2) as counter electrode. Cyclic voltammetry (potential range: 0.3 V to 1.0 V, scan rate: 50mVs^{-1} and 100 mVs^{-1}), differential pulse voltammetry (potential range: 0.3 V to 1.0 V, pulse amplitude: 50 mV, pulse width: 50 ms, increment potential: 4 mV, pulse

period: 500 ms), The ZnO/RGO/ZnO@Zn electrode was utilized as working electrodes.

3. Results and discussion

3.1. Component and morphology determination of ZnO/RGO/ZnO@Zn

The crystallographic structures of ZnO/RGO/ZnO@Zn samples were firstly investigated through XRD patterns. As shown in Fig.1, it is clearly observed those peaks at 36.3^{o}, 38.9^{o}, 42.3^{o}, 54.3^{o}, 70.1^{o}, 70.6^{o} and 77.0^{o} for all the electrodes, which can be attributed to the (002), (100), (101), (102), (103), (110), and (004) planes of metallic Zn (JCPDS No. 04-0831), respectively. These indicate that Zn foil was not consumed completely during the hydrothermal process and thus acted as the current collector of electrode in the following electrochemical tests[24, 25]. The peaks around 31.8^{o}, 34.4^{o}, 36.3^{o}, 47.5^{o}, 56.6^{o}, 62.8^{o}, 67.9^{o} and 69.0^{o}, which is corresponded to the (100), (002), (101), (102), (110), (103), (112), and (201) crystalline planes of the hexagonal ZnO wurtzite structure (JCPDS No. 36-1451)[26]. Furthermore, the broad bump around 25° in XRD pattern verifies the existence of RGO. Therefore, the XRD patterns comfirm the existence of each component of ZnO/RGO/ZnO@Zn nanocomposites.

The presence of RGO and metal oxide in the nanocomposites was also further certified by using Raman spectra. As we can see in the Fig.S1, D-band (1586 cm^{-1}) and G-band (1350 cm^{-1}) are clearly seen in Raman spectra for both RGO and ZnO/RGO/ZnO. Generally speaking, the ratio of D band to G band is usually used to semi-quantitatively determine the reduction level of RGO. In this work, when GO is converted into RGO through the hydrothermal process, a slight increase of the I_D/I_G ratio occurs, indicating that a small decrease in the size of the sp2 domains upon reduction, i.e. RGO has a large quantity of edges[27, 28]. Compared with pure RGO (0.98), a higher I_D/I_G ratio value (1.68) is obtained for the ZnO/RGO/ZnO@Zn electrode, confirming that RGO is further reduced to more disordered structure in the presence of Zinc foil and zinc nitrate. As shown in the inset in Fig.S1, there appear a sharp peak at ~431 cm^{-1} attributed to the vibration mode of E2 and a peak around ~321 cm^{-1} caused by the multiple-phono scattering process, confirming the formation of ZnO nanoparticles in the nanocomposites[26, 29]. Herein, Raman spectra results combined with XRD results verify the existence of RGO and ZnO in the ZnO/RGO/ZnO composite.

The morphology and size of all samples were characterized by FESEM images. As clearly shown in Fig. 2A, nanorod-like ZnO particles are attached on the surface of Zn substrate when only Zn foil was suffered from the process of hydrothermal

reaction. For comparison, in the presence of zinc nitrate, 3D hierarchically spherical ZnO and nanorod-like ZnO are clearly seen in Fig.2B, what's more, the 3D hierarchically spherical ZnO consists of ZnO nanosheets through assembly. In the presence of 15 mg GO, nanorod-like ZnO was converted into cone-shaped nanoparticles ZnO and covered by wrinkled RGO nanosheets, seen in Fig. 2C. In contrast, in the presence of both GO and Zinc nitrate, these 3D hierarchically spherical ZnO are interconnected due to the interaction of RGO and these spherical ZnO particles, seen in Fig. 2D and 2E. As shown in a magnification picture in Fig.2F, it is clearly seen that ZnO nanoparticles are covered by wrinkled RGO and the results confirm the three-decker nanocomposite structure of ZnO/RGO/ZnO@Zn. These indicate that both Zinc nitrate and GO play key roles in controlling the structure and morphology of ZnO/RGO/ZnO@Zn. Furthermore, the elemental mappings in Fig.S2a-d prove that Zn, O and C elements are well uniformly dispersed. The above interconnected 3D hierarchical ZnO/RGO/ZnO@Zn maybe facilitate its sensing capability for sunset yellow.

The detailed information on structure and morphology of ZnO/RGO/ZnO@Zn electrode was further confirmed by TEM. Fig. 3A and 3B show the TEM images of ZnO nanosheets, ZnO nanoparticles and wrinkle RGO of ZnO/RGO/ZnO@Zn, which are well consistent with the results in SEM images. Moreover, the lattice fringes of

0.281 nm and 0.260 nm for ZnO in the HRTEM image (Fig. 3C, D) are well in accordance with the (111) plane and (002) plane of ZnO, respectively. According to the SEM images and TEM images, the synthesis mechanism of ZnO/RGO/ZnO on Zn can be assumed as follows[23]: During the hydrothermal process, based on the chemical redox reaction of reductive Zn foil and oxidative GO, Zn on the outer Zn foil was transformed into ZnO nanoparticles and deposited on the Zn surface, and GO was simultaneously reduced to RGO and covered on the ZnO nanoparticles surface. On the other hand, 3D hierarchical ZnO spheres transformed from Zn ions were attached on the other side of RGO nanosheets because of the electrostatic attraction force between Zn^{2+} and GO.

3.2. Electrocatalytic oxidation of ZnO/RGO/ZnO@Zn electrodes to sunset yellow

The electrocatalytic performances of ZnO/RGO/ZnO@Zn electrode on the sunset yellow species were investigated with differential pulse voltammograms (DPV), cyclic voltammogram (CV) curve in an aqueous solution of 0.2 M phosphate (pH=7.0).

Fig.4A present CV responses of ZnO/RGO/ZnO@Zn, RGO/ZnO@Zn, ZnO@Zn and ZnO/ZnO@Zn in 0.2 M PBS (pH=7.0) solution containing 0.02 mM sunset yellow within the potential range from 0.3 to 1.0 V at a scan rate of 100 mVs^{-1}. Seen

from Fig. 4A, it is clear that the as-prepared ZnO/RGO/ZnO@Zn exhibit an excellent peak current for detecting sunset yellow in comparison with other electrodes, indicating that ZnO/RGO/ZnO@Zn has superior electrocatalytic activity to sunset yellow. The high electrocatalytic response of ZnO/RGO/ZnO@Zn may be mainly ascribed to the synergistic effect of graphene, 3D hierarchically spherical ZnO and cone-shaped ZnO nanoparticles.

Fig.4B shows DPVs of RGO/ZnO@Zn electrode and ZnO/RGO/ZnO@Zn electrode in 0.2 M phosphate buffered solution with (curves (b), (d)) and without 0.01 mM sunset yellow (curves (a), (c)). It is clearly seen that no obvious electrochemical response is observed in the DPV curves for RGO/ZnO@Zn (curve (a)) or ZnO/RGO/ZnO@Zn (curve (c)) in the absence of sunset yellow. For comparison, in the presence of 0.01 mM sunset yellow, the current peak correlated with sunset yellow appears for both RGO/ZnO@Zn (curve (b)) and ZnO/RGO/ZnO@Zn (curve (d)) and the oxidation potential is 0.64 V. What's more, the oxidation current on ZnO/RGO/ZnO@Zn electrode is larger than that of RGO/ZnO@Zn electrode, because ZnO/RGO/ZnO@Zn electrode is loaded with more ZnO nanosheets to prevent the agglomeration of RGO. As a result, the surface area of ZnO/RGO/ZnO@Zn electrode increases and leads to an rise in peak current.

Fig. 4C gives CV curves of ZnO/RGO/ZnO@Zn electrode in 0.2 M phosphate buffered solution(pH=7.0) with (curves (b)) and without 0.01 mM sunset yellow (curves (a)). A pair of visible redox peaks are observed in the presence of 0.01 mM sunset yellow: The oxidation peak at 0.67 V, and the reduction peak at 0.66 V. According to the literature reports [4, 7], the electrochemical redox reaction of sunset yellow is a reversible process (shown in Figure.5). Therefore, the oxidation peak of sunset yellow is 0.67 V, while the reduction peak is 0.66 V. These indicated that the oxidation reaction of sunset yellow occur under the electrocatalytic action of the electrode.

As depicted in Fig. 6A, it shows DPVs of ZnO/RGO/ZnO@Zn electrode in 0.2 M phosphate buffered solution containing various concentrations sunset yellow: (a) 0.01 μM, (b)0.05 μM, (c) 0.5 μM, (d) 1 μM, (e) 2 μM and (f) 5 μM. The phosphate buffer solution of pH=7 was chosen as the optimum condition for the testing of ZnO/RGO/ZnO@Zn electrode. It is obvious that the peak current increases with change of sunset yellow concentration. Furthermore, Fig. 6B displays the calculation curve of the sensor at a sunset yellow concentration of 0.01-5 μM: I_{pa} (μA) = 4.05 C_{SY} (μM L^{-1}) + 4.77 (R^2 =0.997). The sensitivity and detection limit are also determined by calculation: An ultrahigh sensitivity of 20.25 uA·uM^{-1}·cm^{-2} and a limit of detection as low as 3 nM(S/N=3).

Fig.6C present CV curves for ZnO/RGO/ZnO@Zn electrode in 0.2 M phosphate buffer containing 0.01 mM sunset yellow at different scan rates in the range of 20 $mV{\cdot}s^{-1}$ - 200 $mV{\cdot}s^{-1}$. As shown in Fig.6D and Fig.6E, the relation between both the reduction and oxidation peak and the square root of the scan rate ($i \sim v^{1/2}$) is linear, in which the correlation coefficients are 0.995 and 0.999, respectively. Moreover, the linear equation is given as follows: $I_{pa}(\mu A)=1.49v^{1/2}$ -1.74, (R^2=0.995), $I_{pc}(\mu A)$= -1.37$v^{1/2}$ +7.20, (R^2=0.999), which indicates that the redox reaction of sunset yellow on ZnO/RGO/ZnO@Zn electrode is a typical diffusion-controlled electrochemical process.

Table.1 lists some electrochemical sensors for sunset yellow detection reported in previous works. Obviously, as-synthesized ZnO/RGO/ZnO@Zn electrode in this work is superior to other non-enzymatic sunset yellow sensors in some performances including detection limit and linear range on sunset yellow[3, 7, 30-38]. These indicate that ZnO/RGO/ZnO@Zn-based sunset yellow electrochemical sensors has good sensor performance. The superior electrocatalytic performance of ZnO/RGO/ZnO@Zn electrode may be attributed to the synergistic effect of nanocomposites structure. On the one hand, ZnO blocks the aggregation of graphene nanosheets and provides good biocompatibility, the interconnected hierarchical ZnO architecture provides high surface area which facilitates short diffusion distance for

sunset yellow molecules during the electrochemical process. On the other hand, graphene provides good electrical conductivity and catalytic activity. Additional, ZnO/RGO/ZnO@Zn electrode gives a good detection performance for sunset yellow.

In order to evaluate the application of electrodes in the analysis sample, the prepared ZnO/RGO/ZnO@Zn electrode was used as a self-made non-enzymatic sensor to detect the sunset yellow level in fruit juice. The sunset yellow extraction procedure is given as follows: First, take a certain amount of fruit juice and keep it warm for 15 minutes in a water bath at 60℃, and then a small amount of fruit juice was sucked with a micro syringe and diluted with a 0.2 M phosphate buffer solution (pH=7.0). these prepared liquid was subsequently centrifuged at 7000 rpm at 10 min, and the upper layer solution was obtained. At last, the microporous filter membrane with pore diameter of 0.22 μm was used to filter the prepared fruit juice, which was used for the following detection of sunset yellow. Based on the analysis of standard addition method, the content of sunset yellow in fruit juice was 14.83 mg/L. As shown in Table.2, according to the recovery rate in the table, the results of detection confirms the excellent practicability of ZnO/RGO/ZnO@Zn electrode for the detection of sunset yellow.

Besides practicability, the potentially interfering ions coexisting with the sunset yellow in the soft drink were also investigated by DPV method using the optimized

conditions. To study the potentially interfering ions of these species, the concentration of 0.5 μM in 0.2 M PBS (PH=7) of sunset yellow was taken, and then 200-fold concentrations of glucose, vitamin C, citric acid, sucrose, 100-fold concentrations of potassium ion, calcium ion, magnecvsian ion, sodion, ferrous ion, chloridion and 20-fold sudan red, ponceau 4R, allura red, amaranth, tartrazine were added in the solution. Obviously, as shown in Fig.7, the current intensity caused by these potentially interfering ions are so weak and have no significant influence on the response currents of sunset yellow. Therefore, the electrode is suitable to detect sunset yellow in soft drinks.

The long-terms stability of response to sunset yellow for ZnO/RGO/ZnO@Zn electrode is presented in Fig.8, which was tested through DPV technique once a day for ten days in the ambient environment. The retention of 94.7% of the initial response current can be obtained, confirming the excellent stability for longtime application.

The repeatability is another crucial parameter for sensors in the future applications. As shown in Fig. 9, the reproducibility test of ZnO/RGO/ZnO@Zn is carried out in 0.2 M phosphate buffer solution (pH=7.0) by using DPV. A RSD (relative standard deviation) value of 4.2% is obtained based on six

ZnO/RGO/ZnO@Zn electrodes prepared at the same conditions. These indicate that ZnO/RGO/ZnO@Zn electrode as a self-made sensor has an exceptional reproducibility.

4. Conclusions

In summary, a ZnO/RGO/ZnO nanocomposite was in-situ grown on the Zn foil through a Zn foil-involved one-step hydrothermal approach, in which Zn foil acted as support, reductant of GO, Zn source of ZnO in low layer. As-synthesized ZnO/RGO/ZnO@Zn electrode directly served as an electrochemical nonenzymatic sensor, which exhibited excellent sensing performance towards sunset yellow: An ultrahigh sensitivity of 20.25 $uA \cdot \mu M^{-1} \cdot cm^{-2}$, a low limit of detection (3 nM), a wide linear detection ranging from 0.01 to 5 μM and remarkable reproducibility and stability. This work gives a strategy of nonenzymatic sensor on sunset yellow by using metal oxide/RGO-based electrode.

Acknowledgements

We gratefully acknowledge the support by the Shanghai Natural Science Foundation (No. 13ZR1411900), Shanghai Key Laboratory Project (08DZ2230500), Shanghai Leading Academic

Discipline Project (B502) and Opening Project of Shanghai Key Laboratory of New Drug Design (No. 17DZ2271000).

References:

[1] K. Rovina, P.P. Prabakaran, S. Siddiquee, S.M. Shaarani, Methods for the analysis of Sunset Yellow FCF (E110) in food and beverage products- a review, TrAC, Trends Anal. Chem 85 (2016) 47-56.

[2] X. Chen, K. Wu, Y. Sun, X. Song, Highly sensitive electrochemical sensor for sunset yellow based on the enhancement effect of alumina microfibers, Sens. Actuators, B 185 (2013) 582-586.

[3] T. Gan, J. Sun, W. Meng, L. Song, Y. Zhang, Electrochemical sensor based on graphene and mesoporous TiO_2 for the simultaneous determination of trace colourants in food, Food Chem 141(4) (2013) 3731-3737.

[4] J. Wang, B. Yang, H. Wang, P. Yang, Y. Du, Highly sensitive electrochemical determination of Sunset Yellow based on gold nanoparticles/graphene electrode, Anal. Chim. Acta 893 (2015) 41-48.

[5] K.S. Rowe, K.J. Rowe, Synthetic food coloring and behavior: a dose response effect in a double-blind, placebo-controlled, repeated-measures study, J Pediatr 125 (1994) 691-698.

[6] K.S. Minioti, C.F. Sakellariou, N.S. Thomaidis, Determination of 13 synthetic food colorants in water-soluble foods by reversed-phase high-performance liquid chromatography coupled with diode-array detector, Anal. Chim. Acta 583(1) (2007) 103-110.

[7] X. Ye, Y. Du, D. Lu, C. Wang, Fabrication of β-cyclodextrin-coated poly (diallyldimethylammonium chloride)-functionalized graphene composite film modified glassy carbon-rotating disk electrode and its application for simultaneous electrochemical determination colorants of sunset yellow and tartrazine, Anal. Chim. Acta 779 (2013) 22-34.

[8] O. Sha, X. Zhu, Y. Feng, W. Ma, Aqueous two-phase based on ionic liquid liquid-liquid microextraction for simultaneous determination of five synthetic food colorants in different food samples by high-performance liquid chromatography, Food Chem. 174 (2015) 380-386.

[9] J.J. Berzas Nevado, J. Rodriguez Flores, M.J. Villasenor Llerena, N. Rodriguez Farinas, Spectrophotometric resolution of ternary mixtures of Tartrazine, Patent Blue V and Indigo Carmine in commercial products, Anal. Chim. Acta 391(3) (1999) 353-364.

[10] M.S. El-Shahawi, A. Hamza, A.A. Al-Sibaai, A.S. Bashammakh, H.M. Al-Saidi, A new method for analysis of sunset yellow in food samples based on cloud point extraction prior to spectrophotometric determination, J. Ind. Eng. Chem 19(2) (2013) 529-535.

[11] M. Yamada, M. Nakamura, T. Yamada, T. Maitani, Y. Goda, Structural determination of unknown subsidiary colors in food yellow No. 5 (Sunset Yellow FCF), Chem. Pharm. Bull. 44(8) (1996) 1624-1627.

[12] R.A. Medeiros, B.C. Lourencao, R.C. Rocha-Filho, O. Fatibello-Filho, Simultaneous voltammetric determination of synthetic colorants in food using a cathodically pretreated boron-doped diamond electrode, Talanta 97 (2012) 291-297.

[13] S.M. Ghoreishi, M. Behpour, M. Golestaneh, Simultaneous voltammetric determination of Brilliant Blue and Tartrazine in real samples at the surface of a multi-walled carbon nanotube paste electrode, Anal. Methods 3(12) (2011) 2842-2847.

[14] L. Zhao, F. Zhao, B. Zeng, Preparation and application of sunset yellow imprinted ionic liquid polymer - ionic liquid functionalized graphene composite film coated glassy carbon electrodes, Electrochim. Acta 115 (2014) 247-254.

[15] X. Yang, H. Qin, M. Gao, H. Zhang, Simultaneous detection of Ponceat 4R and tartrazine in food using adsorptive stripping voltammetry on an acetylene black nanoparticle-modified electrode, J. Sci. Food Agric. 91(15) (2011) 2821-2825.

[16] J. Li, X. Wang, H. Duan, Y. Wang, Y. Bu, C. Luo, Based on magnetic graphene oxide highly sensitive and selective imprinted sensor for determination of sunset yellow, Talanta 147 (2016) 169-176.

[17] T. Gan, J. Sun, Q. Wu, Q. Jing, S. Yu, Graphene Decorated with Nickel Nanoparticles as a Sensitive Substrate for Simultaneous Determination of Sunset Yellow and Tartrazine in Food Samples, Electroanalysis 25(6) (2013) 1505-1512.

[18] T. Gan, J. Sun, S. Cao, F. Gao, Y. Zhang, Y. Yang, One-step electrochemical approach for the preparation of graphene wrapped-phosphotungstic acid hybrid and its application for simultaneous determination of sunset yellow and tartrazine, Electrochim. Acta 74 (2012) 151-157.

[19] W.S. Hummers, Jr., R.E. Offeman, Preparation of graphitic oxide, J. Am. Chem. Soc. 80 (1958) 1339.

[20] Y. Xu, H. Bai, G. Lu, C. Li, G. Shi, Flexible Graphene Films via the Filtration of Water-Soluble Noncovalent Functionalized Graphene Sheets, J. Am. Chem. Soc. 130(18) (2008) 5856-5857.

[21] S. Min, C. Zhao, Z. Zhang, G. Chen, X. Qian, Z. Guo, Synthesis of $Ni(OH)_2$/RGO pseudocomposite on nickel foam for supercapacitors with superior performance, J. Mater. Chem. A 3(7) (2015) 3641-3650.

[22] S. Wang, P. Ju, Z. Zhu, C. Zhao, Co_3O_4/RGO/Co_3O_4 pseudocomposite grown in situ on a Co foil for high-performance supercapacitors, RSC Adv. 6(102) (2016) 99640-99647.

[23] C. Zhao, X. Wu, P. Li, C. Zhao, X. Qian, Hydrothermal deposition of CuO/rGO/Cu_2O nanocomposite on copper foil for sensitive nonenzymatic voltammetric determination of glucose and hydrogen peroxide, Microchim. Acta 184(7) (2017) 2341-2348.

[24] X. Zhang, J. Dong, X. Qian, C. Zhao, One-pot synthesis of an RGO/ZnO nanocomposite on zinc foil and its excellent performance for the nonenzymatic sensing of xanthine, Sens. Actuators, B 221 (2015) 528-536.

[25] C. Zhao, X. Wu, X. Zhang, P. Li, X. Qian, Facile synthesis of layered CuS/RGO/CuS nanocomposite on Cu foam for ultrasensitive nonenzymatic detection of glucose, J. Electroanal. Chem. 785 (2017) 172-179.

[26] X. Dong, Y. Cao, J. Wang, M.B. Chan-Park, L. Wang, W. Huang, P. Chen, Hybrid structure of zinc oxide nanorods and three dimensional graphene foam for supercapacitor and electrochemical sensor applications, RSC Adv. 2(10) (2012) 4364-4369.

[27] J. Yan, Z. Fan, W. Sun, G. Ning, T. Wei, Q. Zhang, R. Zhang, L. Zhi, F. Wei, Advanced Asymmetric Supercapacitors Based on $Ni(OH)_2$/Graphene and Porous Graphene Electrodes with High Energy Density, Adv. Funct. Mater. 22(12) (2012) 2632-2641.

[28] G.-T. Liu, H.-F. Chen, G.-M. Lin, P.-p. Ye, X.-P. Wang, Y.-Z. Jiao, X.-Y. Guo, Y. Wen, H.-F. Yang, One-step electrodeposition of graphene loaded nickel oxides nanoparticles for acetaminophen detection, Biosens. Bioelectron. 56 (2014) 26-32.

[29] J.F. Scott, Uv resonant Raman scattering in zinc oxide, Phys. Rev. B 2(4) (1970) 1209-1211.

[30] S. Rouhani, Novel Electrochemical Sensor for Sunset Yellow Based on a Platinum Wire-Coated Electrode, Anal. Lett. 42(1) (2009) 141-153.

[31] S.M. Ghoreishi, M. Behpour, M. Golestaneh, Simultaneous determination of Sunset yellow and Tartrazine in soft drinks using gold nanoparticles carbon paste electrode, Food Chem. 132(1) (2012) 637-641.

[32] Y.-Z. Song, Electrochemical reduction of sunset yellow at a multiwalled carbon nanotube (MWCNT)-modified glassy carbon electrode and its analytical application, Can. J. Chem. 88(7) (2010) 676-681.

[33] M.R. Majidi, R. Fadakar Bajeh Baj, A. Naseri, Carbon Nanotube–Ionic Liquid (CNT–IL) Nanocamposite Modified Sol-Gel Derived Carbon-Ceramic Electrode for Simultaneous Determination of Sunset Yellow and Tartrazine in Food Samples, Food Analytical Methods 6(5) (2013) 1388-1397.

[34] X. Qiu, L. Lu, J. Leng, Y. Yu, W. Wang, M. Jiang, L. Bai, An enhanced electrochemical platform based on graphene oxide and multi-walled carbon nanotubes nanocomposite for sensitive determination of Sunset Yellow and Tartrazine, Food Chem. 190 (2016) 889-895.

[35] Y. Ya, C. Jiang, T. Li, J. Liao, Y. Fan, Y. Wei, F. Yan, L. Xie, Y. Ya, C. Jiang, T. Li, J. Liao, Y. Fan, Y. Wei, F. Yan, L. Xie, A Zinc Oxide Nanoflower-Based Electrochemical Sensor for Trace Detection of Sunset Yellow, Sensors 17(3) (2017).

[36] D. Sun, C. Xu, J. Long, T. Ge, Determination of Sunset Yellow using a carbon paste electrode modified with a nanostructured resorcinol-formaldehyde resin, Microchim. Acta 182(15-16) (2015) 2601-2606.

[37] L. Yu, M. Shi, X. Yue, L. Qu, A novel and sensitive hexadecyltrimethyl ammonium bromide functionalized graphene supported platinum nanoparticles composite modified glassy carbon electrode for determination of sunset yellow in soft drinks, Sens. Actuators, B 209 (2015) 1-8.

[38] M. Wang, J. Zhao, Facile synthesis of Au supported on ionic liquid functionalized reduced graphene oxide for simultaneous determination of Sunset yellow and Tartrazine in drinks, Sens. Actuators, B 216 (2015) 578-585.

Figure Captions

Fig.1 XRD patterns of pure Zn, ZnO@Zn, ZnO/ZnO@Zn, RGO/ZnO@Zn and ZnO/RGO/ZnO@Zn.

Fig.2 SEM images of ZnO@Zn (A), ZnO/ZnO@Zn (B), RGO/ZnO@Zn (C), ZnO/RGO/ZnO@Zn (D, E,F).

Fig. 3 (A, B) TEM images of ZnO nanosheets, ZnO nanoparticles and fold RGO, (C, D) HRTEM image of a ZnO in ZnO/RGO/ZnO@Zn nanocoposite.

Fig.4 (A) CV responses of ZnO/RGO/ZnO@Zn, RGO/ZnO@Zn, ZnO@Zn and ZnO/ZnO@Zn in 0.2 M PBS (pH=7.0) solution containing 0.02 mM sunset yellow at 100 mVs^{-1}. (B) DPVs of RGO/ZnO/Zn foil ((a),(b))and ZnO/RGO/ZnO@Zn foil ((c),(d)) in 0.2 M phosphate buffered with ((b), (d)) or without ((a),(c)) 0.01 mM sunset yellow. (C) CVs of ZnO/RGO/ZnO@Zn foil in PBS with (b) or without 0.01 mM sunset yellow (a) at 50 mVs^{-1}

Fig.5 The electrochemical redox reaction of sunset yellow.

Fig.6 (A) DPVs of ZnO/RGO/ZnO@Zn electrode in 0.2 M pH=7.0 phosphate buffer solution containing various concentrations of sunset yellow: (a) 0.01μM, (b) 0.05 μM, (c) 0.5 μM, (d) 1 μM, (e) 2μM and (f) 5 μM. (B) Calibration plot of ZnO/RGO/ZnO@Zn electrode at sunset yellow concentration of 0.01–5 μM. **(C)** CV curves of ZnO/RGO/ZnO@Zn electrode in 0.2 M pH=7.0 phosphate buffer solution containing 0.01 mM sunset yellow at different scan rates (from a-j: 20-

200 mVs^{-1}). (D) and (E) the plots of the redox peak currents versus the square root of the scan rate ($i \sim v^{1/2}$).

Fig.7 Selectivity of ZnO/RGO/ZnO@Zn electrode.

Fig.8 Long-terms stability of ZnO/RGO/ZnO@Zn electrode response to sunset yellow for ten days.

Fig.9 The reproducibility test in 0.2 M phosphate buffer solution (pH=7.0) for ZnO/RGO/ZnO@Zn electrode.

Scheme

Scheme 1 Schematic illustration for the synthesis and electrochemical reaction mechanism of the ZnO/RGO/ZnO@Zn electrode

Table

Table.1 Comparison of the proposed electrode with other electrodes used for determining sunset yellow.

Table.2 Application of the as-prepared electrode in determining sunset yellow in the soft drink.

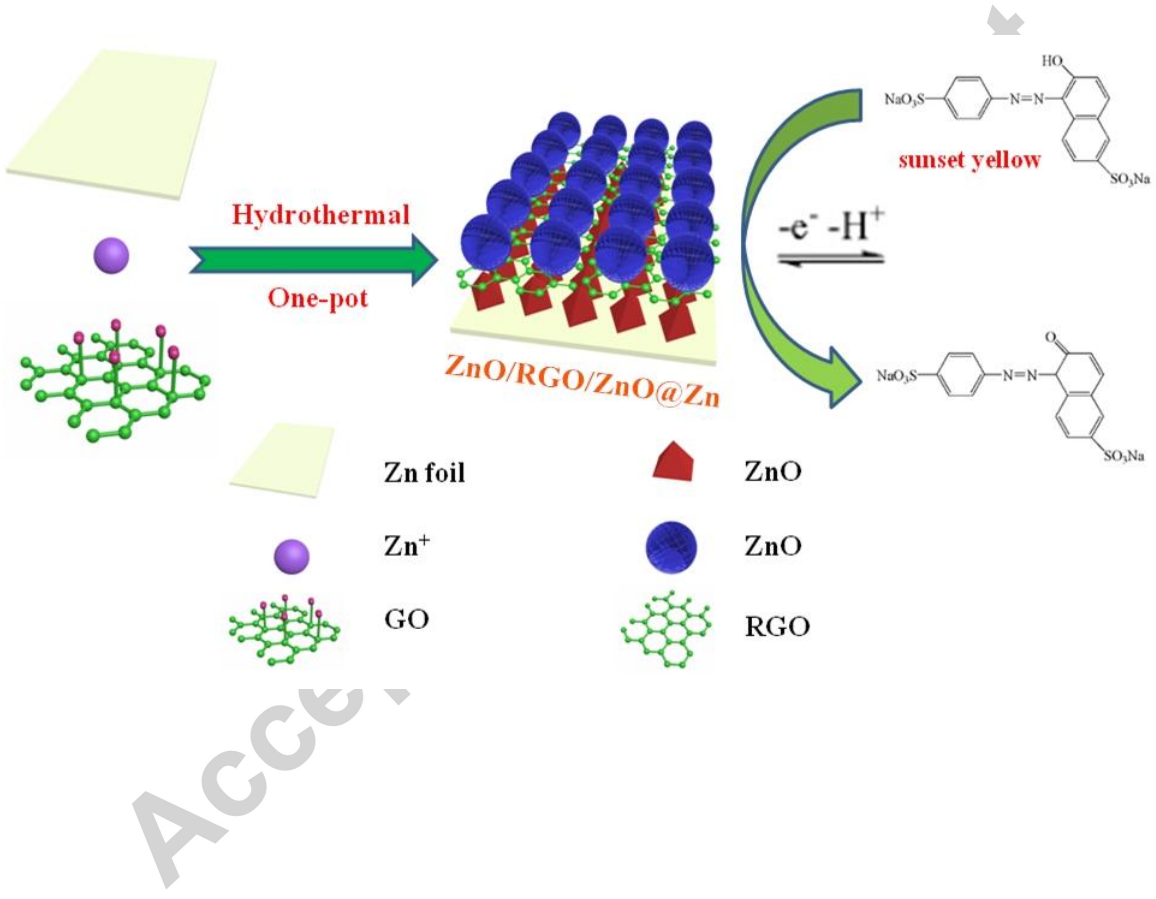
Hydrothermal
One-pot
ZnO/RGO/ZnO@Zn
-e⁻ -H⁺
sunset yellow
Zn foil
Zn⁺
GO
ZnO
ZnO
RGO

Scheme 1

Table.1

Electrode material	Linear range(μM)	Detection limit(nM)	Ref.
CN/TiO_2-CPE	0.02-2.05	6	[3]
	0.02-1.18	8	
β-CD-PDDA-Gr/Gc-RDE	0.05-20	12.5	[7]
Pt/GCE	0.0316-3.16	31.6	[30]
Au NPs/CPE	0.1-2.0	30	[31]
MWCNT/GCE	2.65-276	1100	[32]
MWCNTs-IL/GCE	0.4-110	100	[33]
RGO/MWCNT	0.09-8.0	25	[34]
ZnONF	0.0011-0.022 0.022-0.154	0.22	[35]
Nanostructured RF resin	0.0003-0.125	0.09	[36]
CTAB-Gr-Pt/GCE	0.08-10	4.2	[37]
ILRGO-Au	0.004-1	0.52	[38]
ZnO/RGO/ZnO foil	0.05-5	3	This work

Table.2

Sample	Added(μM)	Found(μM)	Recovery
1	1	4.55	109.5%
2	2	5.58	99.29%
3	3	7.17	98.62%

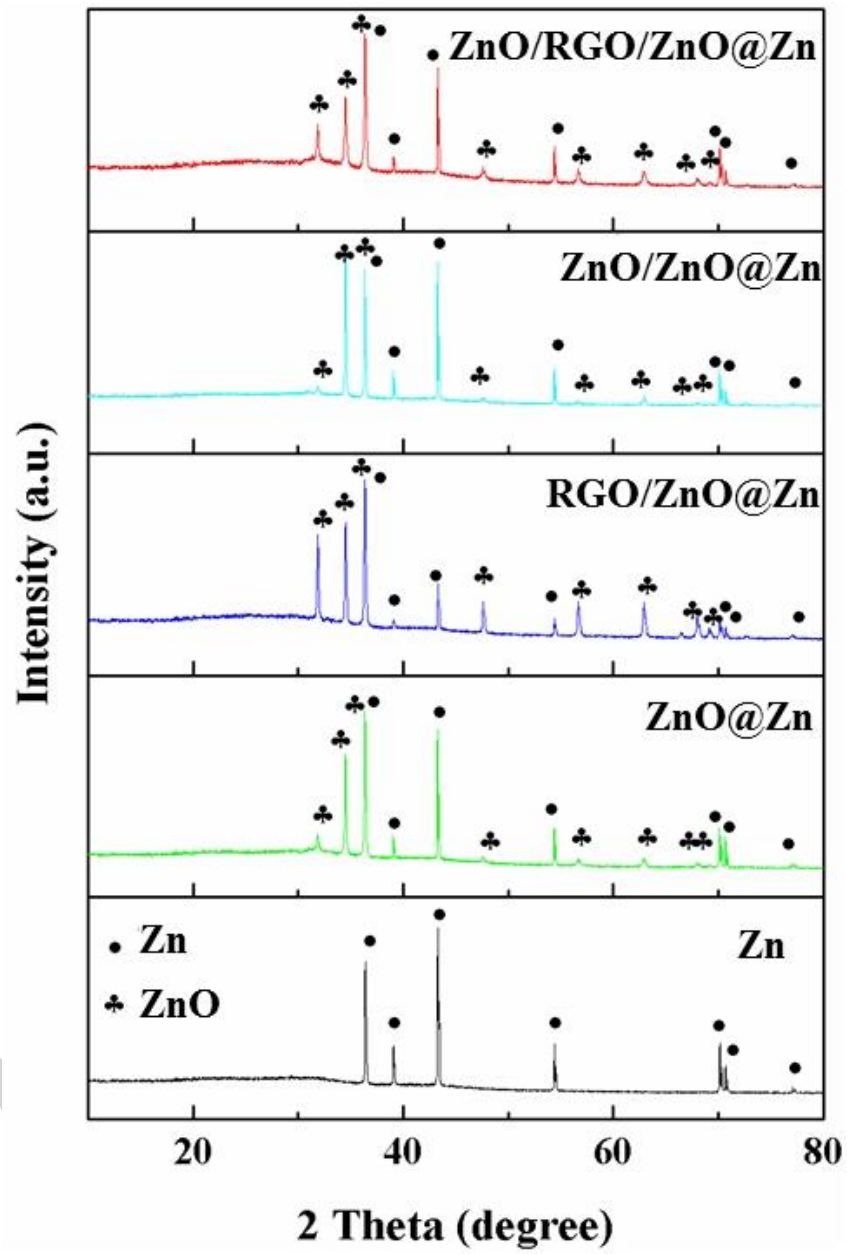
ZnO/RGO/ZnO@Zn
ZnO/ZnO@Zn
RGO/ZnO@Zn
ZnO@Zn
Zn
Zn
ZnO
Intensity (a.u.)
20
40
60
80
2 Theta (degree)

Fig. 1

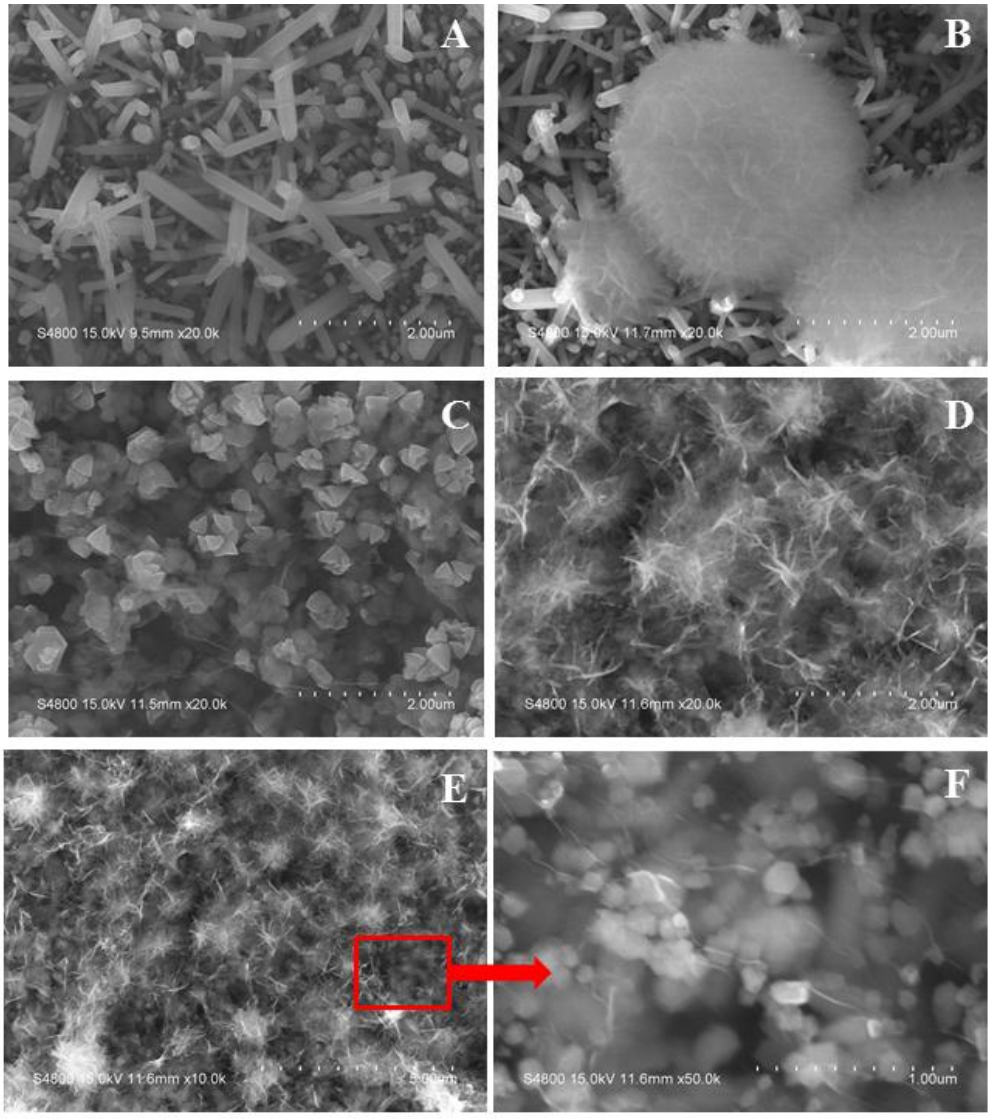
A
S4800 15.0kV 9.5mm x20.0k
2.00um
B
2.00um
C
S4800 15.0kV 11.5mm x20.0k
2.00um
D
S4800 15.0kV 11.6mm x20.0k
2.00um
E
F
S4800 15.0kV 11.6mm x50.0k
1.00um

Fig. 2

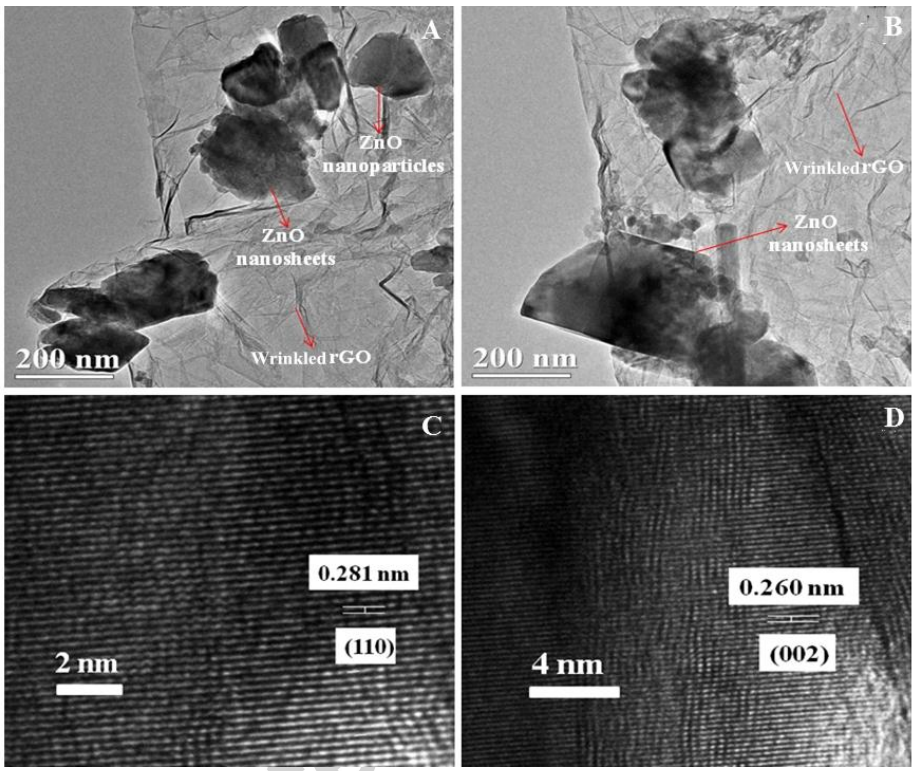

Fig. 3

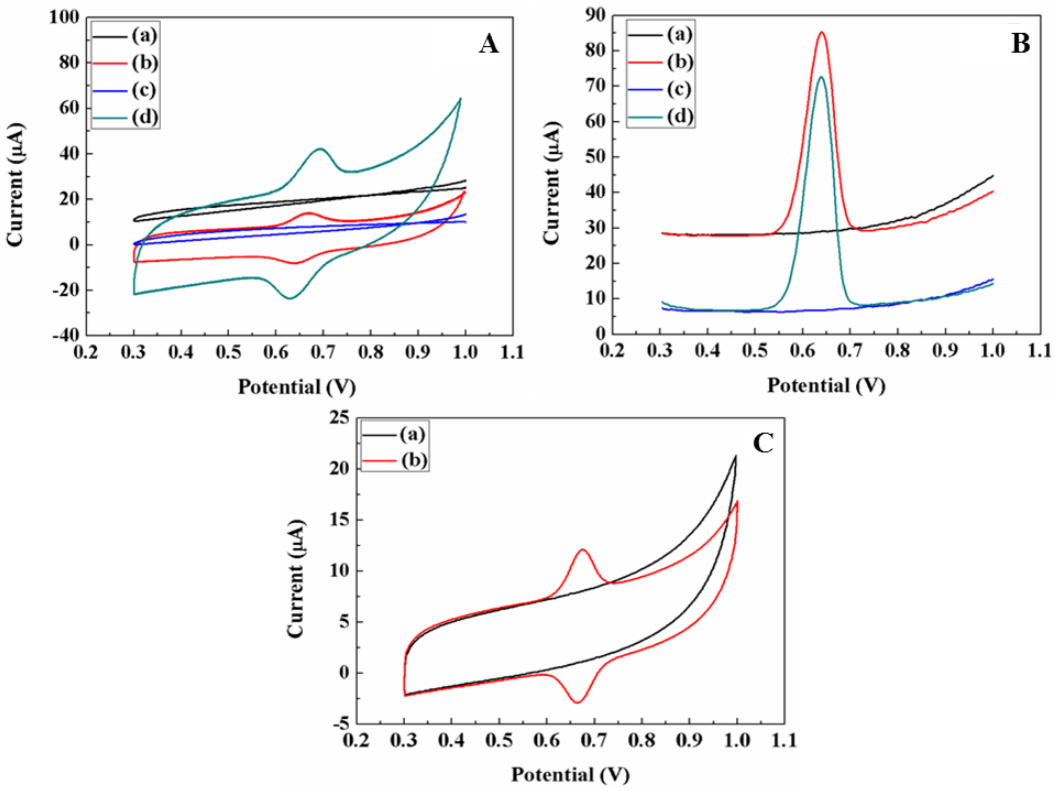
A
(a)
(b)
(c)
(d)
Current (μA)
Potential (V)
B
(a)
(b)
(c)
(d)
Current (μA)
Potential (V)
C
(a)
(b)
Current (μA)
Potential (V)

Fig. 4

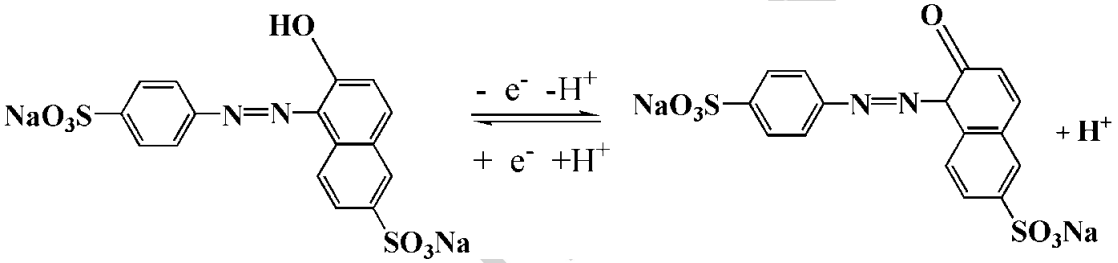

Fig. 5

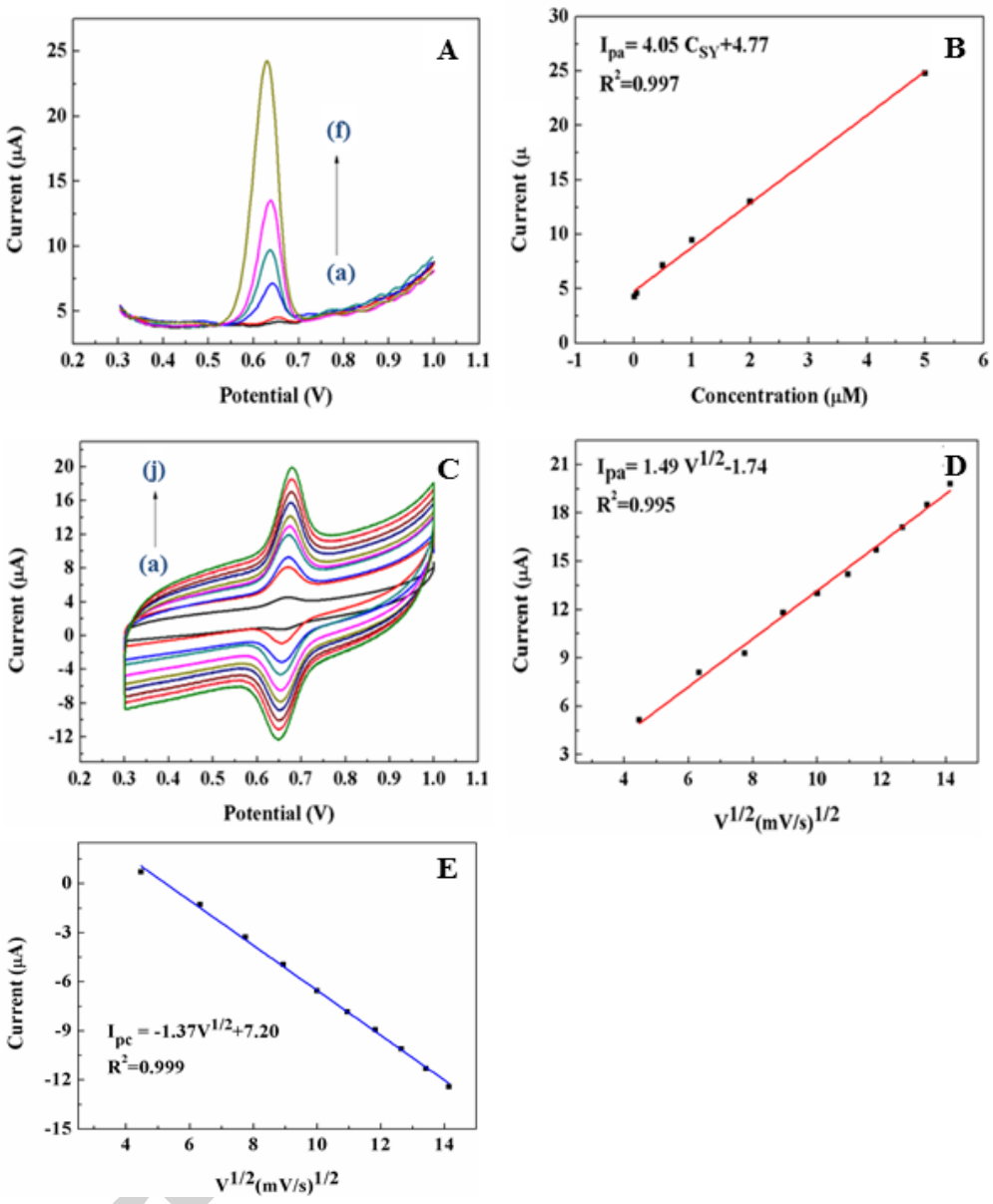
A
(f)
(a)
Current (μA)
Potential (V)
B
I_{pa}= 4.05 C_{SY}+4.77
R^2=0.997
Current (μ
Concentration (μM)
C
(j)
(a)
Current (μA)
Potential (V)
D
I_{pa}= 1.49 $V^{1/2}$-1.74
R^2=0.995
Current (μA)
$V^{1/2}(mV/s)^{1/2}$
E
I_{pc} = -1.37$V^{1/2}$+7.20
R^2=0.999
Current (μA)
$V^{1/2}(mV/s)^{1/2}$

Fig. 6

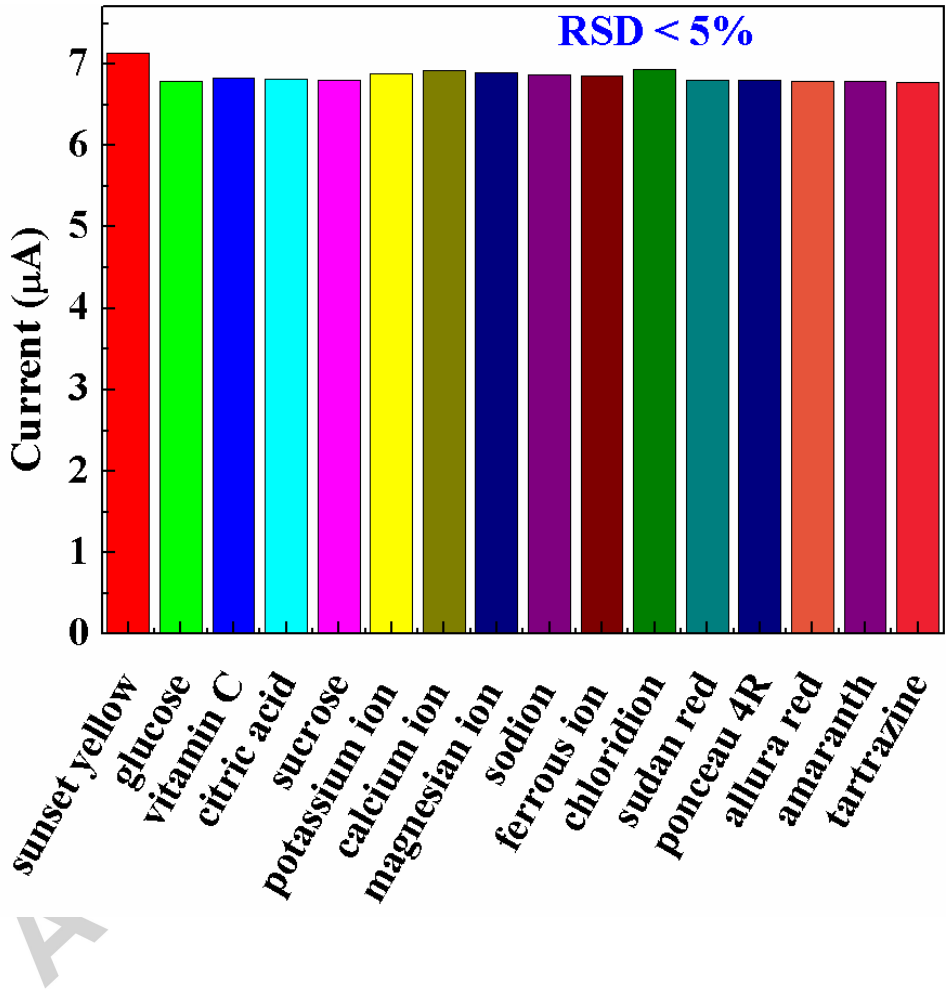
RSD < 5%
Current (μA)
0
1
2
3
4
5
6
7
sunset yellow
glucose
vitamin C
citric acid
sucrose
potassium ion
calcium ion
magnesian ion
sodion
ferrous ion
chloridion
sudan red
ponceau 4R
allura red
amaranth
tartrazine

Fig.7

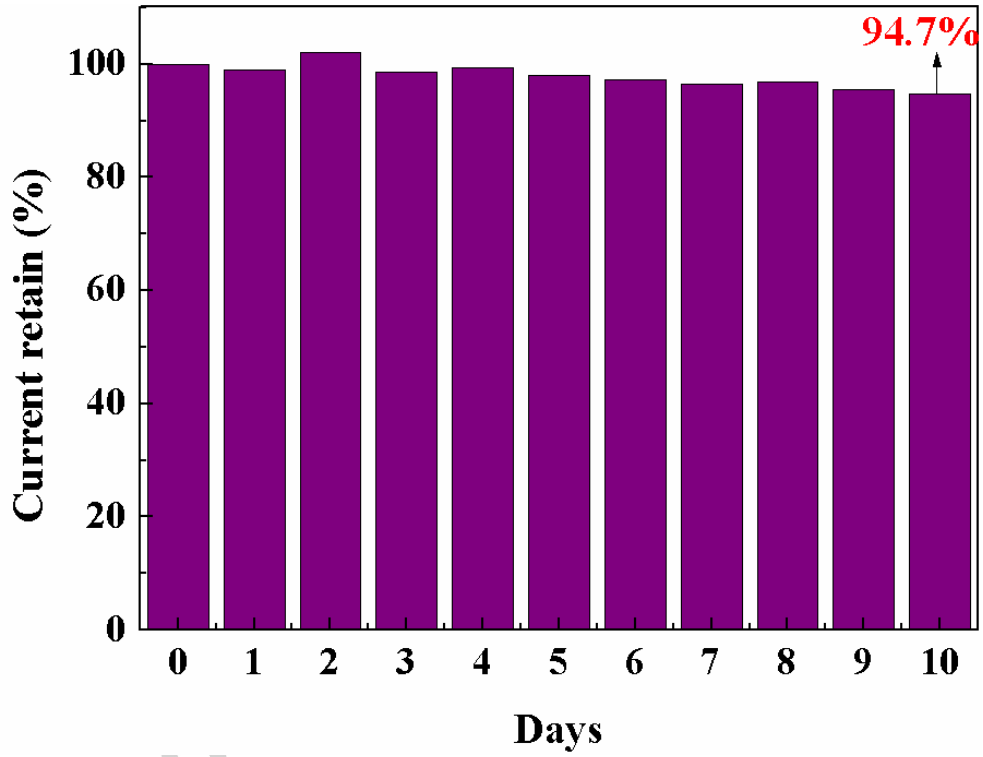

Fig.8

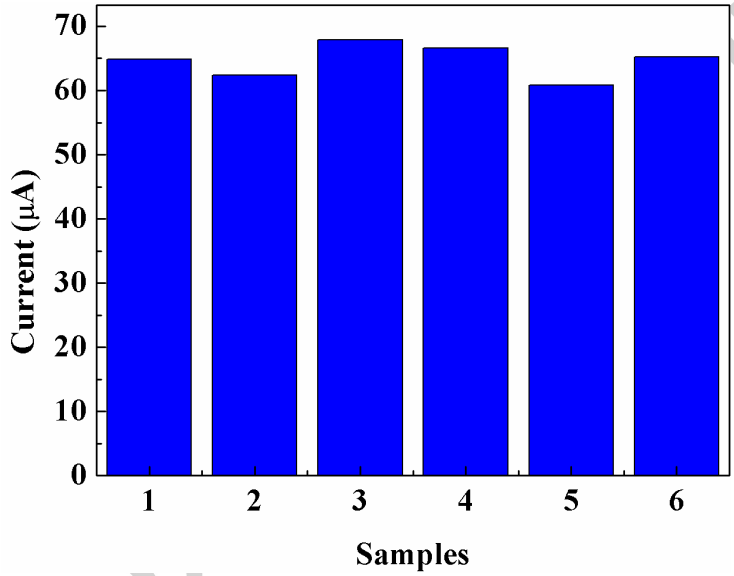

Fig. 9

Highlights

- A ZnO/RGO/ZnO nanocomposite *in-situ* grown on Zn foil through a Zn foil-involved hydrothermal reaction.

- Zn foil as support, Zn source of ZnO, reductant of GO and the subsequent current collector.
- GO play a key role in controlling morphology and structure of the composites.
- Ultrahigh-sensitivity and low detection limit for sunset yellow.